

Solar Energetic Particle Spectrum on 13 December 2006 Determined by IceTop

R. Abbasi,²⁰ M. Ackermann,³² J. Adams,¹¹ M. Ahlers,²⁴ J. Ahrens,²¹ K. Andeen,²⁰
 J. Auffenberg,³¹ X. Bai,²³ M. Baker,²⁰ B. Baret,⁹ S.W. Barwick,¹⁶ R. Bay,⁵
 J.L. Bazo Alba,³² K. Beattie,⁶ T. Becka,²¹ J.K. Becker,¹³ K.H. Becker,³¹ P. Berghaus,²⁰
 D. Berley,¹² E. Bernardini,³² D. Bertrand,⁸ D.Z. Besson,¹⁸ J.W. Bieber,²³ E. Blaufuss,¹²
 D.J. Boersma,²⁰ C. Boehm,²⁶ J. Bolmont,³² S. Böser,³² O. Botner,²⁹ J. Braun,²⁰ D. Breder,³¹
 T. Burgess,²⁶ T. Castermans,²² D. Chirkin,²⁰ B. Christy,¹² J. Clem,²³ D.F. Cowen,^{27,28}
 M.V. D'Agostino,⁵ M. Danninger,¹¹ A. Davour,²⁹ C.T. Day,⁶ C. De Clercq,⁹ L. Demirörs,¹⁷
 O. Depaeppe,⁹ F. Descamps,¹⁴ P. Desiati,²⁰ G. de Vries-Uiterweerd,³⁰ T. DeYoung,²⁸
 J.C. Diaz-Velez,²⁰ J. Dreyer,¹³ J.P. Dumm,²⁰ M.R. Duvoort,³⁰ W.R. Edwards,⁶
 R. Ehrlich,¹² J. Eisch,²⁰ R.W. Ellsworth,¹² O. Engdegard,²⁹ S. Euler,¹ P.A. Evenson,²³
 O. Fadiran,³ A.R. Fazely,⁴ K. Filimonov,⁵ C. Finley,²⁰ M.M. Foerster,²⁸ B.D. Fox,²⁸
 A. Franckowiak,⁷ R. Franke,³² T.K. Gaisser,²³ J. Gallagher,¹⁹ R. Ganugapati,²⁰
 L. Gerhardt,⁶ L. Gladstone,²⁰ A. Goldschmidt,⁶ J.A. Goodman,¹² R. Gozzini,²¹ D. Grant,²⁸
 T. Griesel,²¹ A. Gross,¹⁵ S. Grullon,²⁰ R.M. Gunasingha,⁴ M. Gurtner,³¹ C. Ha,²⁸
 A. Hallgren,²⁹ F. Halzen,²⁰ K. Han,¹¹ K. Hanson,²⁰ D. Hardtke,⁵ R. Hardtke,²⁵
 Y. Hasegawa,¹⁰ J. Heise,³⁰ K. Helbing,³¹ M. Hellwig,²¹ P. Herquet,²² S. Hickford,¹¹
 G.C. Hill,²⁰ K.D. Hoffman,¹² K. Hoshina,²⁰ D. Hubert,⁹ J.P. Hülss,¹ P.O. Hulth,²⁶
 K. Hultqvist,²⁶ S. Hundertmark,²⁶ R.L. Imlay,⁴ M. Inaba,¹⁰ A. Ishihara,¹⁰ J. Jacobsen,²⁰
 G.S. Japaridze,³ H. Johansson,²⁶ J.M. Joseph,⁶ K.H. Kampert,³¹ A. Kappes,^{20,33} T. Karg,³¹
 A. Karle,²⁰ H. Kawai,¹⁰ J.L. Kelley,²⁰ J. Kiryluk,^{5,6} F. Kislak,³² S.R. Klein,^{5,6} S. Klepser,³²
 G. Kohnen,²² H. Kolanoski,⁷ L. Köpke,²¹ M. Kowalski,⁷ T. Kowarik,²¹ M. Krasberg,²⁰
 K. Kuehn,¹⁶ T. Kuwabara,²³ M. Labare,⁸ K. Laihem,¹ H. Landsman,²⁰ R. Lauer,³²
 H. Leich,³² D. Leier,¹³ A. Lucke,⁷ J. Lundberg,²⁹ J. Lünemann,¹³ J. Madsen,²⁵
 R. Maruyama,²⁰ K. Mase,¹⁰ H.S. Matis,⁶ C.P. McParland,⁶ K. Meagher,¹² A. Meli,¹³
 M. Merck,²⁰ T. Messarius,¹³ P. Mészáros,^{27,28} H. Miyamoto,¹⁰ A. Mohr,⁷ T. Montaruli,^{20,34}
 R. Morse,²⁰ S.M. Movit,²⁷ K. München,¹³ R. Nahnauer,³² J.W. Nam,¹⁶ P. Niessen,²³
 D.R. Nygren,⁶ S. Odrowski,³² A. Olivas,¹² M. Olivo,²⁹ M. Ono,¹⁰ S. Panknin,⁷ S. Patton,⁶
 C. Prez de los Heros,²⁹ J. Petrovic,⁸ A. Piegsa,²¹ D. Pieloth,³² A.C. Pohl,^{29,35} R. Porrata,⁵
 N. Potthoff,³¹ J. Pretz,¹² P.B. Price,⁵ G.T. Przybylski,⁶ R. Pyle,²³ K. Rawlins,²
 S. Razzaque,^{27,28} P. Redl,¹² E. Resconi,¹⁵ W. Rhode,¹³ M. Ribordy,¹⁷ A. Rizzo,⁹
 W.J. Robbins,²⁸ J. Rodrigues,²⁰ P. Roth,¹² F. Rothmaier,²¹ C. Rott,²⁸ C. Roucelle,^{5,6}
 D. Rutledge,²⁸ D. Ryckbosch,¹⁴ H.G. Sander,²¹ S. Sarkar,²⁴ K. Satalecka,³²
 S. Schlenstedt,³² T. Schmidt,¹² D. Schneider,²⁰ O. Schultz,¹⁵ D. Seckel,²³ B. Sembrugg,³¹
 S.H. Seo,²⁶ Y. Sestayo,¹⁵ S. Seunarine,¹¹ A. Silvestri,¹⁶ A.J. Smith,¹² C. Song,²⁰
 G.M. Spiczak,²⁵ C. Spiering,³² T. Stanev,²³ T. Stezelberger,⁶ R.G. Stokstad,⁶
 M.C. Stoufer,⁶ S. Stoyanov,²³ E.A. Strahler,²⁰ T. Straszheim,¹² K.H. Sulanke,³²
 G.W. Sullivan,¹² Q. Swillens,⁸ I. Taboada,⁵ O. Tarasova,³² A. Tepe,³¹ S. Ter-Antonyan,⁴
 S. Tilav,²³ M. Tluczykont,³² P.A. Toale,²⁸ D. Tosi,³² D. Turcan,¹² N. van Eijndhoven,³⁰
 J. Vandenbroucke,⁵ A. Van Overloop,¹⁴ V. Viscomi,²⁸ C. Vogt,¹ B. Voigt,³² C. Walck,²⁶
 T. Waldenmaier,²³ H. Waldmann,³² M. Walter,³² C. Wendt,²⁰ S. Westerhoff,²⁰
 N. Whitehorn,²⁰ C.H. Wiebusch,¹ C. Wiedemann,²⁶ G. Wikström,²⁶ D.R. Williams,²⁸
 R. Wischniewski,³² H. Wissing,¹ K. Woschnagg,⁵ X.W. Xu,⁴ G. Yodh,¹⁶ and S. Yoshida¹⁰

Corresponding author E-mail evenson@udel.edu

1. Introduction

The IceTop air shower array now under construction at the South Pole as the surface component of the IceCube neutrino telescope (Achterberg et al. 2006) detected an unusual near-solar-minimum Ground Level Enhancement (GLE) after a solar flare on 13 December 2006. Beginning at 0220

UT, the 4B class flare occurred at solar coordinates S06 W24, accompanied by strong (X3.4) X-ray emission and type II and IV radio bursts. The LASCO coronagraph on the SOHO spacecraft observed a halo CME launch from the Sun at ~ 0225 UT with speed estimated to be ~ 1770 km/s. We have begun (Bieber et al. 2007) a comprehensive analysis of the propagation of solar energetic particles in this event. However the focus of this Letter is the new and unique ability of IceTop to derive the energy spectrum of these particles in the multi-GeV regime from a single detector with a well defined viewing direction.

When completed, IceTop will have approximately 500 square meters of ice Cherenkov collecting area arranged in an array of 80 stations on a 125 m triangular grid to detect air showers from one PeV to one EeV. Each station consists of two, two meter diameter tanks filled with ice to a depth of 90 cm. Tanks are instrumented with two Digital Optical Modules (DOM) operated at different gain settings to provide appropriate dynamic range to cover both large and small air showers. Each DOM contains a 10 inch photomultiplier and an advanced readout system capable of digitizing the full waveform. For historical reasons, the two discriminator counting rates recorded in each DOM are termed SPE (Single Photo Electron), and MPE (Multi Photo Electron). In the present analysis the SPE threshold corresponds approximately to 20 photoelectrons (PE), and the MPE threshold to 100 PE.

Due to the high altitude (2835m) and the nearly zero geomagnetic cutoff at the South Pole, secondary particle spectra at the detector retain a significant amount of information on the spectra of the primary particles. In a thin, ionization detector these secondary particles either would not interact, or would produce virtually indistinguishable signals. This is not the case in the thick IceTop detector, where a traversing muon produces 130 PE and the typical electron only 15 PE. Signal amplitude therefore carries information about the composition and spectra of the incident particles, albeit integrated over broad regions of the spectrum. In particular, differences in counting rates of discriminators at different thresholds allow us to infer the particle spectrum incident at the top of the atmosphere.

¹III Physikalisches I., RWTH Aachen U., D-52056 Aachen

²Physics & Astronomy, U. Alaska Anchorage, AK 99508

³CTSPS, Clark-Atlanta U., Atlanta, GA 30314

⁴Physics, Southern U., Baton Rouge, LA 70813

⁵Physics, U. California, Berkeley, CA 94720

⁶Lawrence Berkeley National Laboratory, Berkeley, CA 94720

⁷I. für Physik, Humboldt-Universität zu Berlin, D-12489 Berlin

⁸Science Faculty CP230, U. Libre de Bruxelles, B-1050 Brussels

⁹Vrije U. Brussel, Dienst ELEM, B-1050 Brussels

¹⁰Physics, Chiba U., Chiba Japan 263-8522

¹¹Physics & Astronomy, U. Canterbury, Christchurch NZ

¹²Physics, U. Maryland, College Park, MD 20742

¹³Physics, Universität Dortmund, D-44221 Dortmund

¹⁴Subatomic and Radiation Physics, U. Gent, B-9000 Gent

¹⁵MPI für Kernphysik, D-69177 Heidelberg

¹⁶Physics and Astronomy, U. California, Irvine, CA 92697

¹⁷High Energy Physics, École Poly Fédérale, CH-1015 Lausanne

¹⁸Physics and Astronomy, U. Kansas, Lawrence, KS 66045

¹⁹Astronomy, U. Wisconsin, Madison, WI 53706

²⁰Physics, U. Wisconsin, Madison, WI 53706

²¹Institute of Physics, U. Mainz, D-55099 Mainz

²²U. Mons-Hainaut, B-7000 Mons

²³Physics & Astronomy & BRI, U. Delaware, Newark, DE 19716

²⁴Physics, U. Oxford, Oxford OX1 3NP

²⁵Physics, U. Wisconsin, River Falls, WI 54022

²⁶Physics, Stockholm U., SE-10691 Stockholm

²⁷Astronomy & Astrophysics, PA State, Univ. Park, PA 16802

²⁸Physics, PA State, Univ. Park, PA 16802

²⁹High Energy Physics, Uppsala U., S-75121 Uppsala

³⁰Physics & Astronomy, Utrecht U./SRON, NL-3584 Utrecht

³¹Physics, U. Wuppertal, D-42119 Wuppertal

³²DESY, D-15735 Zeuthen

³³Phys. Inst., U. Erlangen-Nürnberg, D-91058 Erlangen

³⁴Fisica, U. Bari, I-70126 Bari

³⁵Pure & Applied Sciences, Kalmar U., S-39182 Kalmar

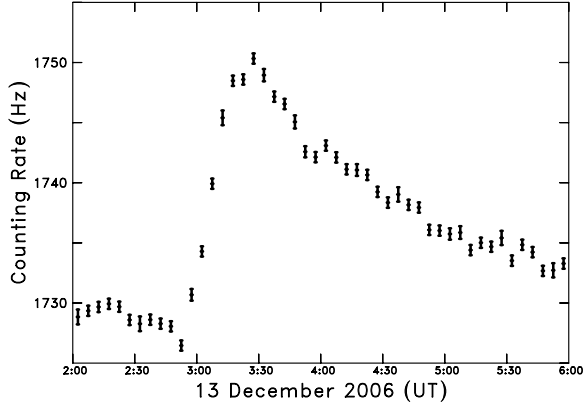


Fig. 1.— Average Single Photo Electron (SPE) discriminator counting rate in IceTop prior to and during the solar particle event of 13 December 2006. Data are averaged over five minute intervals.

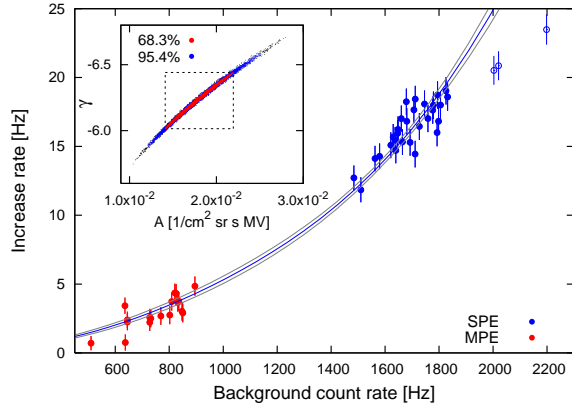


Fig. 2.— Increase of individual IceTop discriminator counting rates averaged from 0320UT to 0410UT over that during a reference interval (0115UT to 0255UT) plotted against counting rate during the reference interval. Bars indicate statistical errors. Blue line is the best fit to a power law (in rigidity) spectrum, AP^γ . Gray lines give the one sigma error band on the spectrum as discussed in the text. Three discriminators (open symbols) showed anomalous behavior and were excluded as described in the text. The insert illustrates correlation of error estimates for the fit parameters (A, γ).

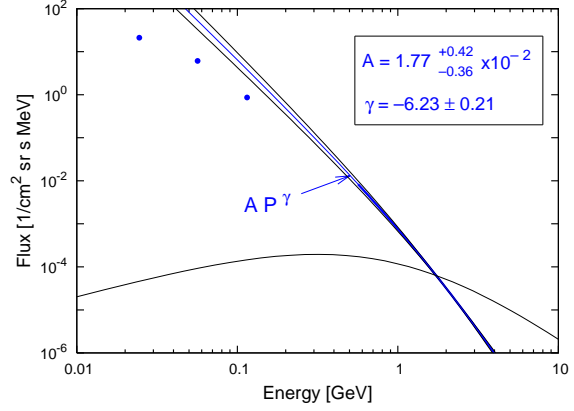


Fig. 3.— IceTop proton spectrum from the fit in Figure 2 (heavy blue line with one sigma error band). The black line is the assumed background cosmic ray proton spectrum and the points are the maximum proton fluxes from GOES spacecraft data.

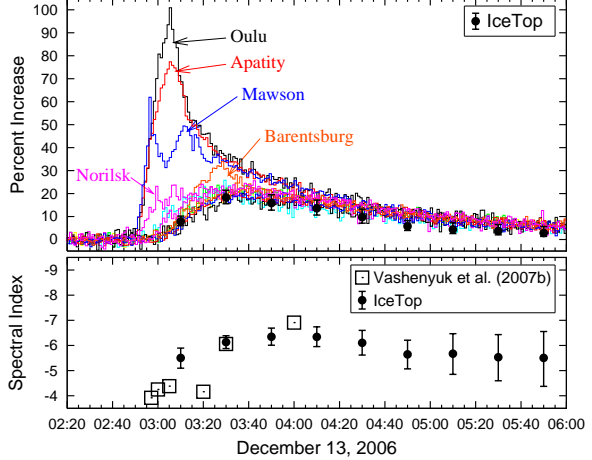


Fig. 4.— (Top) Calculated increase in a sea level neutron monitor based on the IceTop spectrum (heavy black circles) compared with the counting rate of several near sea level neutron monitors. Traces for Oulu, Apatity, Mawson, Norilsk and Barentsburg are labelled while those for Cape Schmidt, Fort Smith, Inuvik, Nain, Peawanuck, Tixie Bay, and Thule are not. (Bottom) Spectral index from IceTop compared to that of Vashenyuk et al. (2007b)

2. Observations

On 13 December 2006, IceTop was returning useful data from 32 SPE and 15 MPE discriminators operating in 16 tanks. Figure 1 shows the average SPE discriminator counting rate as a function of time with a pronounced increase due to the arrival of solar particles. In Figure 2 we focus on the time interval 0320 to 0410 where the spectral shape (see below) is essentially constant. We plot the additional counting rate (due to the solar particles) for individual discriminators as a function of counting rate prior to the onset of the solar particle fluxes. IceTop was in test mode with all discriminators set at nominal, uncalibrated thresholds. Fortunately this produced a significant gap between MPE and SPE count rates, as well as a modest range of true thresholds within each group. To derive an energy spectrum from these data we had to deal simultaneously with the unknown element composition of the particles (primarily the solar proton/alpha ratio) and the lack of a detector calibration.

Yield functions, with units area-solid-angle, describe the relation between particle flux at the top of the atmosphere and the occurrence rate of a specified signal. For IceTop they depend on the arrival direction, rigidity (P) and mass of the primary nucleus and on the discriminator setting which determines the light level required to count a particle. At high latitudes such as South Pole defocusing in the geomagnetic field produces an isotropic flux at the top of the atmosphere even if the flux outside the magnetosphere is highly anisotropic. At low energy (when the probability of a particle or its progeny to reach the surface is small), the yield function is smaller than the physical area-solid-angle of the tank, but at high energy (when a shower can give rise to a signal even if the trajectory of the primary passes outside the tank) it is larger.

By definition, the convolution of a yield function $S_{pe}(P)$ with a particle spectrum $J(P)$ gives the counting rate above the corresponding pe threshold. The product of the yield function and the spectrum is termed the response function. Thus, at time t during the solar flare the counting rate of the i th discriminator, with threshold $pe(i)$,

is

$$N_i(t) = \sum_k \int S_{pe(i)}^k(P) \{J_k(P) + \Delta J_k(P, t)\} dP, \quad (1)$$

where $J(P)$ is the steady state cosmic-ray spectrum, $\Delta J(P, t)$ is the additional flux of particles at time t during the event, and the summation is over particle species. Note that by interchanging summation and integration the concept of a single response function representing a composite spectrum is well defined.

Using FLUKA (Fasso et al. 1993), and measured cosmic ray composition and spectra appropriate to solar minimum, we generated galactic cosmic ray (GCR) response functions for several different thresholds, which could be interpolated to produce response functions for arbitrary thresholds. Lacking a calibration, we integrated the response functions to predict the background counting rate for each possible threshold, then assigned to each discriminator the response function that exactly predicted the observed counting rates during the reference interval 0115UT to 0255UT.

Most derivations of a solar spectrum (e.g. Bombardieri et al. (2006)) assume the particles to be all protons and construct a proton yield function from GCR response functions (e.g. Lockwood & Debrunner (1999)). Composition at these energies has never actually been measured, so we make the much simpler assumption that the composition is galactic, constructing yield functions by dividing the interpolated GCR response functions by a modified force field proton spectrum (see Figure 3; Caballero-Lopez & Moraal (2004); Clem et al. (2004)). If solar particles are proton rich compared to galactic, these yield functions produce a lower limit on the solar proton spectrum. We estimate that for an all proton composition the true intensity would be ~ 1.2 times this limit.

With this set of yield functions we minimized χ^2 for a power law (in rigidity) spectrum. The actual fit is shown in Figure 2. The minimum was 1.5 per degree of freedom, confirming the visual impression that some of the deviation from the fit is due to inherent differences among the detectors. Results from a Monte Carlo simulation are presented in an insert, with the parameter pair resulting from each realization plotted as a point.

The 68.3% of the realizations producing the lowest χ^2 are indicated in red; we take this to define the one sigma error range of the parameters. Due to the high correlation we do not discuss the errors on the parameters separately. The error band shown is the *envelope* of all possibilities within the 68.3% contour. Three discriminators (open symbols in Figure 2) were excluded from the fit primarily because their background counting rates stand so far outside the cluster of discriminators operating under the same nominal conditions. Correlation of their background count rate with barometer reading over the three day interval surrounding the flare event was also anomalous compared to that of the other discriminators.

The derived IceTop spectrum is shown in Figure 3 by the blue curve, with the heavier line denoting the energy range that contributes substantially (tenth to ninetieth percentile) to the fit. The parameter ranges quoted correspond to the dashed rectangle in Figure 2. The overshoot of the spectral extrapolation compared to low energy proton fluxes from the GOES spacecraft is rather typical, and is generally interpreted as a steepening of the spectrum over the intervening energy range. Note that IceTop is able to derive the spectrum of a small increase over a large background. An increase of this magnitude would not be statistically resolved with a detector of a size practical for flight on a spacecraft or balloon.

3. Interpretation

Repeating this analysis on 20 minute subsets of the data, and using a published response function (Moraal et al. 1989) we calculated (Figure 4) the expected count rate increase for a sea level neutron monitor. The error bars were determined, as in Figure 2, as the range of allowed values from parameter pairs within a 68.3% contour. If, instead, we were to compute the standard deviation over all realizations in the Monte Carlo simulation, the error bars would be a factor ~ 0.65 smaller. For comparison we show one minute averages of the counting rates of several near sea level neutron monitors. Particles first arrived from the sunward direction, observed best by Oulu, Mawson, and Apatity in a very tight beam focused by the interplanetary magnetic field (Bieber et al. 2007). The initial rise was seen by Mawson, then the beam

moved over to Oulu and Apatity, before briefly switching back toward Mawson. By the time Barentsburg saw the beam, nearly isotropic scattered particles were beginning to dominate the flux. The viewing direction of IceTop was similar to that of monitors that primarily observed backscattered particles. We consider the agreement of our calculation with the observations from these monitors to be rather good, given that we arguably have no free parameters.

Traditional methods for determining energy spectra rely on observations from pairs or groups of stations with different geomagnetic cutoff and station altitude (Lockwood et al. 2002; Ryan et al. 2005; Bombardieri et al. 2006) which typically have strongly energy dependent viewing directions. Such an analysis has been reported for the 13 December 2006 event by Vashenyuk et al. (2007a,b) who employ the world network of neutron monitors to achieve a range of viewing directions and geomagnetic cutoffs under the common assumption that the event can be modelled by a function separable in energy and anisotropy. In the lower panel of Figure 4 we compare the spectral index derived from both analyses. Late in the event, when the fluxes are more isotropic, the agreement is excellent. Early on, Vashenyuk et al. (2007b) derived a significantly harder overall spectrum than ours, and also reported a pronounced softening of the spectrum with time. In contrast, our analysis yielded a nearly constant spectral index. We believe that the discrepancy results from the way Vashenyuk et al. (2007b) parameterized the anisotropy. As a result, their fit confuses anisotropy evolution with spectral evolution. We are confident that we eventually will converge on a common understanding when the precise spectrum derived from IceTop is properly included as a constraint on the fit. When definitive results from the PAMELA spacecraft instrument are available they should also contribute greatly to a comprehensive analysis. It is also clear that future results from IceTop will be greatly enhanced by the neutron monitor network, which will continue to be the primary source of information on anisotropy.

4. Future Plans for IceTop

Encouraged that such a straightforward analysis of IceTop data yields a useful picture of the

time dependent spectrum of the solar particle event on 13 December 2006, we are working to better understand the instrumentation to reduce systematic uncertainties. We are also reconfiguring IceTop to increase statistical precision. DOMs are being reprogrammed to collect and transmit histograms, with ten second resolution, of the integrated charge signal for all events that trigger the MPE discriminators. These will then be set to trigger at a rate of approximately 2000 Hz, a limit determined by the tolerable dead time of the system for air shower studies. Each of the (eventual) 160 high gain DOMs will thus return a spectrum that is statistically equivalent to the spectrum returned by the entire ensemble of DOMs employing the present data collection method. SPE discriminators will be set at a variety of thresholds to populate the regime at rates higher than 2000 Hz, probably up to about 10,000 Hz. DOMs are capable of accumulating histograms at these higher rates, but the dead time would be unacceptable for normal operation. Overall we should be able to achieve a sensitivity two orders of magnitude greater than current neutron monitors for event detection.

These changes will dramatically improve the energy resolution of IceTop for determining solar flare spectra. In Figure 2, there is some spread within the two clusters of points but not enough to go much beyond a two parameter fit. With properly spaced coverage and extensions out to 10,000 Hz, we will be able to measure spectral curvatures or cutoffs. We are indeed looking forward to the coming solar maximum.

We acknowledge the support from the following agencies: National Science Foundation Office of Polar Programs; National Science Foundation Physics Division; University of Wisconsin Alumni Research Foundation; Department of Energy; National Energy Research Scientific Computing Center (supported by the Office of Energy Research of the Department of Energy); NSF-supported TeraGrid system at the San Diego Supercomputer Center (SDSC); National Center for Supercomputing Applications (NCSA); Swedish Research Council; Swedish Polar Research Secretariat; Knut and Alice Wallenberg Foundation; German Ministry for Education and Research; Deutsche Forschungsgemeinschaft (DFG); Fund

for Scientific Research (FNRS-FWO); Flanders Institute to encourage scientific and technological research in industry (IWT); Belgian Federal Science Policy Office; Netherlands Organisation for Scientific Research (NWO); M. Ribordy: SNF (Switzerland); A. Kappes: EU Marie Curie OIF Program; T. Kuwabara and J. W. Bieber: NASA grants NNX07AH73G and NNX08AQ18G. We thank our colleagues at IZMIRAN, Polar Geophysical Institute (Russia), and Australian Antarctic Division for furnishing neutron monitor data.

REFERENCES

- Achterberg, A. et al. 2006, *Astroparticle Physics*, 26, 155
- Bieber, J.W., & P. Evenson, *Proc. 24th Int. Cosmic Ray Conf.*, 1995, 4, 1316
- Bieber, John W. et al. 2007, *Proc. 30th Int. Cosmic Ray Conf.*, paper 0376 in press
- Bombardieri, D.J., M.L. Duldig, K.J. Michael & J. E. Humble 2006, *ApJ*, 644, 565
- Caballero-Lopez, R. A. & H. Moraal 2004 *J. Geophys. Res.*, 109, A01101
- Clem, J.M, G. De Angelis, P. Goldhagen & J. W. Wilson 2004, *Radiation Protection Dosimetry*, 110(1-4), 423
- Fassò, A. et al. 1993, *NIM-A*, 332(3), 459
- Lockwood, J.A. & H. Debrunner 1999, *Space Sci. Rev.* 88, 483
- Lockwood, J.A., H. Debrunner, E.O. Flückiger & J.M. Ryan 2002, *Sol. Phys.*, 208, 113
- Moraal, H., M.S. Potgieter, P.H. Stoker & A.J. van der Walt 1989, *J. Geophys. Res.*, 94, 1459
- Ryan, J. & Milagro Collaboration 2005, *Proc. 29th Int. Cosmic Ray Conf.*, 1, 245
- Vashenyuk, E.V., Y.V. Balabin & P.H. Stoker 2007a, *Adv. Space Res.*, 40, 331
- Vashenyuk, E.V. et al. 2007b, *Proc. 30th Int. Cosmic Ray Conf.*, paper 0362 in press